Int J Thermophys (2011) 32:974–983
DOI 10.1007/s10765-011-0961-7

Simultaneous Measurements of Thermal Properties of Individual Carbon Fibers

Jianli Wang · Bai Song · Xing Zhang · Yang Song · Gangping Wu

Received: 12 October 2010 / Accepted: 5 March 2011 / Published online: 8 April 2011

Abstract Combining the steady-state and quasi-steady-state T type probes, the longitudinal thermal conductivity and thermal effusivity of individual mesophase pitch-based carbon fiber heat treated at 2800 °C and 1000 °C have been measured from 100 K to 300 K. The present method allows simultaneous measurements of thermal properties using the same instrument, by simply changing the applied direct current to alternating current. The specific heat is found to decrease with increasing heat-treatment temperature and to approach the value of graphite. The highly graphitized carbon fiber has a maximum thermal conductivity of 410 $W \cdot m^{-1} \cdot K^{-1}$ at about 250 K, and its thermal diffusivity decreases with increasing temperature. Comparatively, the thermal conductivity of the fiber heat treated at 1000 °C is much smaller, with the peak shifting to high temperature due to a large defect density, and its thermal diffusivity is nearly temperature independent.

Keywords Carbon fiber · Heat-treatment temperature · Specific heat · T type probe · Thermal conductivity

J. Wang · B. Song · X. Zhang (✉)
Department of Engineering Mechanics, Key Laboratory for Thermal Science and Power Engineering of Ministry of Education, Tsinghua University, Beijing 100084, China
e-mail: x-zhang@tsinghua.edu.cn

J. Wang
School of Mechanical Engineering, Jiangsu Key Laboratory for Design and Manufacture of Micro/Nano Biomedical Instruments, Southeast University, Nanjing 210096, China

Y. Song · G. Wu
Institute of Coal Chemistry, Chinese Academy of Sciences, Taiyuan 030001, China

1 Introduction

The extraordinary properties of carbon fiber have promoted wide applications in electrode, nuclear reactor, aerospace, sports, and etc. [1]. The carbon fiber derived from mesophase pitch has been recognized as a promising material for applications requiring a high heat transfer rate due to its excellent thermal properties. Therefore, the measurement of thermal properties, including the thermal conductivity and thermal diffusivity, is critically important to design practical devices. From a fundamental point of view, the thermal properties can be used to investigate its structural defects and phonon–phonon interactions [2], thus adding to our knowledge of the microstructure, which is closely related to the manufacturing process, including polymerization, spinning, oxidation, carbonization, and graphitization [3].

Several techniques have been developed to measure the thermal conductivity and thermal diffusivity of carbon fiber [2,4–12]. For the thermal-conductivity measurement, Raman spectroscopy is a powerful technique, which is also applied to characterize the crystalline perfections [4]. For the thermal-diffusivity measurement, the alternating current calorimetric method [5], the Angstrom method [6], and some noncontact techniques have been applied [8,10]. Comparatively, reports on the specific heat of carbon fiber are limited. Recently, Pradere et al. [10] measured separately the thermal diffusivity and specific heat of carbon fiber from 700 K to 2500 K by applying their previous techniques, and the specific heat was found to decrease as the heat-treatment temperature (HTT) increased. Rhim et al. [11] measured the thermal conductivity and thermal diffusivity of carbon fiber using the laser-flash method from 373 K to 1273 K, and found first a decrease of the specific heat with increasing HTT until about 1000 K and later an increase with HTT. However, below room temperature, no reliable technique so far was able to simultaneously measure the thermal conductivity and thermal diffusivity of such a fine fiber with a diameter of 10 μm or less.

By combining the steady-state and quasi-steady-state T type probes [7,13], we measure both the longitudinal thermal conductivity and thermal diffusivity of individual mesophase pitch-based carbon fiber heat treated at temperatures of 2800 °C and 1000 °C, based on which, the relationship between the thermal properties and the microstructure is systematically investigated.

2 Microstructures of Carbon Fiber

X-ray powder diffraction (XRD, D/MAX-TTR III) was used to study the microstructure of carbon fiber, and three standard parameters were determined, including d_{002}, Lc, and La. d_{002} corresponds to the interlayer spacing between the neighboring hexagonal carbon layers; La and Lc are the crystallite size parallel and perpendicular to the hexagonal carbon layers, respectively. For graphitizing carbon [14], when the HTT was above 1700 °C, graphitization increased rapidly with increasing temperature [15,16]. Hamada et al. [15] found that d_{002} and $Lc(002)$ were almost constant when the HTT was below 1200 °C. When the HTT was above 2000 °C, $Lc(002)$ increased linearly with HTT, while d_{002} decreased monotonically. Figure 1 shows XRD spectra for

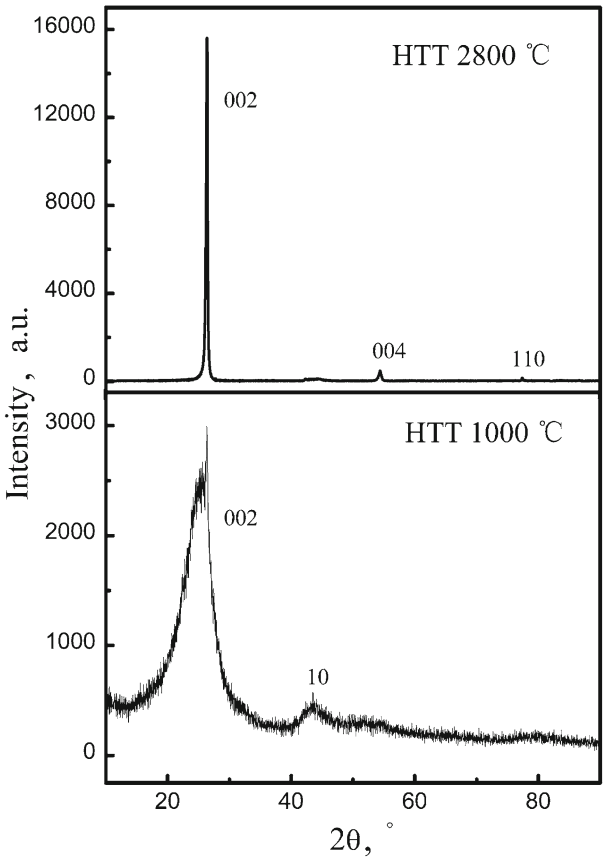

Fig. 1 X-ray powder patterns for carbon fibers heat treated at 2800 °C and 1000 °C

the test carbon fibers. Compared with 1000 °C heat-treated fiber, the (002) diffraction profile for 2800 °C heat-treated fiber is sharper and narrower, and a weaker background noise is also observed, indicating more amorphous phases are converted to ordered phases [16]. The presence of two-dimensional reflection, labeled (10), in the XRD pattern of the fiber heat treated at 1000 °C indicates the non-regularity in the direction normal to graphene layer planes. The interlayer spacing d_{002} is calculated from the diffraction angle of the (002) peak, and the crystallite sizes, *Lc*(002) and *La*(110), are determined using the Scherrer equation from the full width at half-maximum intensity of the (002) and (110) reflections, respectively.

The transverse textures of the fibers were observed by a high resolution high spatial scanning electron microscope (SEM, JSM-6301F) with both low and high magnifications, and more than 95 mass% carbon was found in both fibers by energy dispersive X-ray spectroscopy (EDS). SEM photographs of the carbonized fibers show that the cross sections are ribbon-shaped. A slight pleated structure can be detected from the fiber heat treated at 1000 °C, as shown in Fig. 2c and d. For the highly graphitized fiber, the cross section is clearly made of sheet-like graphene layer planes, indicating a higher degree of preferred orientation than that of the former, as shown in Fig. 2a

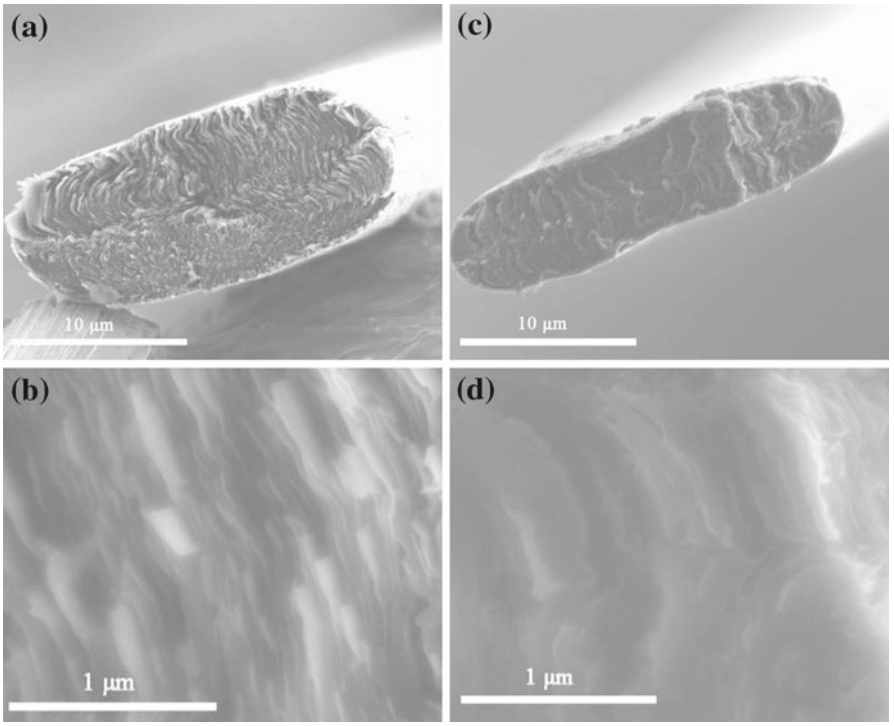

Fig. 2 SEM photographs from the transverse texture of carbon fibers. (a) and (b) show low and high magnifications of fiber heat treated at 2800 °C, and (c) and (d) show low and high magnifications of fiber heat treated at 1000 °C

Table 1 Microstructural characterization of mesophase pitch-based carbon fibers

Fiber samples	XRD properties (nm)			EDS properties (mass%)		Cross section (μm)	
	d_{002}	*Lc*(002)	*La*(110)	C	O	Length	Width
HTT 2800 °C	0.3375	28.2	40.0	96.78	3.22	21.6	8.3
HTT 1000 °C	0.344	1.4	–	97.96	2.04	21.8	6.0

and b. A summary of the microstructural parameters determined by XRD and SEM is given in Table 1.

3 Methods

The experimental setup is shown in Fig. 3. The carbon fiber was located in a vacuum chamber, which was continuously evacuated by a vacuum pump and a molecular pump to obtain a vacuum level of 10^{-3} Pa. The four-wire technique was applied to measure the voltage across the hot wire, and the four terminals were connected to the electrical circuit in either dotted box I or that in dotted box II. The thermal conductivity can be determined using the steady-state T type probe [7], with the electrical circuit shown

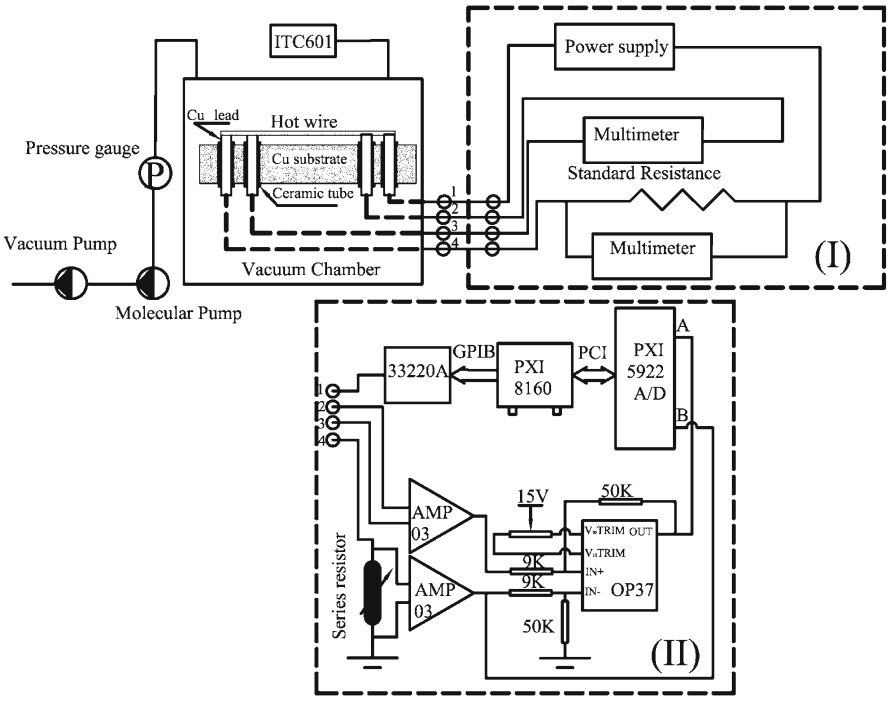

Fig. 3 Measurement systems: the carbon fiber is placed in a vacuum chamber, four terminals are connected to the electrical circuits for the steady-state experiment as in dotted box I or that for the quasi-steady-state experiment as in dotted box II

in dotted box I. In the T type probe, a short Pt wire serves simultaneously as a thermometer and a heater, which is subjected to a direct current. If both ends of the Pt wire are ideally heat sunk to the substrate, a parabolic temperature distribution will be formed along the Pt wire. When the free end of fiber is connected to the midpoint of the Pt wire with an interstitial material, using the same amount of Joule heating, the temperature of the Pt wire is reduced because some heat will conduct out through the test fiber. Thus, measurements of the average temperature rise of the Pt wire with and without the attached fiber allow us to determine the total thermal resistance due to the introduction of the test fiber. In this experiment, fine platinum black powder was used as the interstitial material, and the thermal contact resistance of the junction between the fiber and the Pt wire was ignored. Due to the large aspect ratio, the radiation heat loss from the fiber surface has a large effect on the experimental results. As a consequence, the relationship between the total thermal resistance introduced by the attached fiber and its thermal conductivity can be expressed as

$$\phi(l_{\mathrm{f}}) = \frac{\tanh\left(\sqrt{\pi h_{\mathrm{f}} D_{\mathrm{f}} R_{\mathrm{f}}}\right)}{\sqrt{\pi h_{\mathrm{f}} D_{\mathrm{f}} R_{\mathrm{f}}}} R_{\mathrm{f}} \tag{1}$$

where D_{f} is the equivalent fiber diameter, h_{f} is the heat transfer coefficient, calculated by $h_{\mathrm{f}} \approx 4\varepsilon_{\mathrm{f}}\sigma T_0^3$, with the test temperature T_0, Stefan–Boltzmann constant σ, and

emissivity ε_f be 0.9 for fiber [11], R_f is the thermal resistance of the fiber, defined by $R_f = l_f/(S_f\lambda_f)$, with fiber length l_f, cross-sectional area S_f, and thermal conductivity λ_f. Other details can be found in previous work [7], therefore are not discussed here.

In the same T type probe configuration, the thermal effusivity of carbon fiber can be measured when an alternating current is imposed on the Pt wire [13]. The thermal effusivity is defined by

$$b_f = \sqrt{C_v\lambda_f} = \frac{\lambda_f}{\sqrt{\alpha_f}} \tag{2}$$

where C_v is the volumetric specific heat and α_f is the thermal diffusivity. In the classical 3ω method [17], an alternating current at a frequency 1ω passing through the Pt wire will create a temperature fluctuation at 2ω, which further causes 3ω voltage across the wire. The obtained 3ω voltage is related to the thermal properties of the Pt wire and the surrounding materials. Prior to contacting the test fiber, the thermal conductivity and thermal diffusivity of the Pt wire are calibrated using the self-heating 3ω method [18]. After introducing the carbon fiber, the 3ω voltages are measured again, and the thermal impedance introduced by the fiber can be expressed as

$$\chi(l_f) = \frac{S_h}{S_f}\left(\frac{b_f^2}{b_h^2} - i\frac{2h_f\lambda_f}{\omega D_f b_h^2}\right)^{-\frac{1}{2}} + (1+i)\frac{\sqrt{2}}{2}\mu\frac{FR_c}{R_h} \tag{3}$$

where $\mu = l_h(2\omega/\alpha_h)^{0.5}$, subscripts h and f denote the Pt wire and test fiber, respectively. Due to the presence of the platinum black powder, the differential thermal impedance of the junction between the Pt wire and the test fiber is taken to be the product of the steady-state thermal resistance, R_c, and a ratio function, F. For this quasi-steady-state experiment, the differential thermal impedance of the platinum black junction can no longer be ignored [19], and F is found to be negative. At a heating frequency of 0.1 Hz to 1 Hz, previous studies [13,19] confirmed that the best-fit thermal effusivity using Eq. 3 was independent of the thermal impedance of the platinum black junction, because the thermal diffusion length of the interstitial material was thermally thin, so that the corresponding F was frequency independent. The radiation heat loss contributes to the imaginary part in the first bracket in Eq. 3, which increases with decreasing frequency and the equivalent diameter of the test wire. Considering the radiation heat loss effect, the thermal conductivity of carbon fiber should be measured in advance using the steady-state T type probe.

In the quasi-steady-state experiment, as shown in dotted box II, a function generator 33220A supplied the driving voltage, a series resistor with precision of 0.001 Ω was used to balance the 1ω voltage of the hot wire, and the voltage across the resistor was connected to input channel B of an A/D board (PXI 5922) to get the driving current. The voltage across the hot wire was first adjusted by the series resistor, and then pre-amplified by a homemade circuit before connecting to the input channel A of the A/D board. The detected signals were finally analyzed in an industrial computer (PXI 8106) using a Labview-based virtual lock-in. It was very convenient to change the applied direct current to alternating current, so that the thermal conductivity

and thermal effusivity of the same fiber could be determined under the condition that the test temperature and high vacuum environment were maintained the same during the entire measurement, and the thermal diffusivity and volumetric specific heat of the test fiber were calculated based on Eq. 2.

4 Results and Discussion

Using the steady-state T type probe, the temperature dependence of the longitudinal thermal conductivity is shown in Fig. 4. At room temperature, the thermal conductivity of the fiber heat treated at 2800 °C is about 30 times larger than that of the fiber heat treated at 1000 °C, and a different temperature dependence behavior is also observed. For the highly graphitized fiber, the thermal conductivity increases with increasing temperature, and reaches a maximum value of 410 $\mathrm{W \cdot m^{-1} \cdot K^{-1}}$ at about 250 K. Comparatively, the thermal conductivity of the other fiber increases monotonically with increasing temperature and shows no clear sign of a maximum in the test temperature range, so the peak of thermal conductivity is shifted to higher temperature as the HTT decreases, as observed in vapor-grown fibers [4]. Since heat transport in carbon fibers is dominated by phonons, the peak shift of the thermal conductivity can be explained by the phonon diffusion model. The thermal conductivity parallel to the graphene layer plane can be expressed as

$$\lambda = L \sum_{\mathrm{p}} \langle \upsilon_{\mathrm{p}} \rangle \cdot S_{\mathrm{p}} \tag{4}$$

where S_{p} is the heat capacity per unit volume due to mode p, $\langle \upsilon_{\mathrm{p}} \rangle$ is the mean effective velocity for lattice vibrations, which is often simply taken to be constant, and L is the phonon mean free path, which consists of two contributions: $L^{-1} = L_{\mathrm{ph-ph}}^{-1} + L_{\mathrm{ph\text{-}def}}^{-1}$, $L_{\mathrm{ph-ph}}$ and $L_{\mathrm{ph\text{-}def}}$ are the scattering lengths due to the phonon–phonon umklapp collisions and phonon-defect collisions, respectively. Below the peak, L is limited by phonon scattering against defects. Since $L_{\mathrm{ph\text{-}def}}$ is in general taken to be temperature independent, the thermal conductivity increases with increasing temperature due to an increase of heat capacity. Above the peak, the phonon–phonon umklapp scattering becomes stronger, and the thermal conductivity decreases as the temperature increases due to the rapid decreasing $L_{\mathrm{ph-ph}}$. The maximum thermal conductivity occurs roughly where $L_{\mathrm{ph-ph}} \sim L_{\mathrm{ph\text{-}def}}$ [20]. Since the density of defects in carbon fiber increases with decreasing HTT, $L_{\mathrm{ph\text{-}def}}$ is typically small for the fiber heat treated at low temperature, so that the maximum thermal conductivity will occur with a small $L_{\mathrm{ph-ph}}$, indicating a high temperature.

Figure 5 shows the temperature dependence of the thermal effusivity measured by the quasi-steady-state experiment. The thermal effusivity is found to vary linearly with temperature from 100 K to 300 K for both fibers, and the fiber with a high HTT obviously gives a larger value and a steeper slope than the other one, revealing that the thermal effusivity can be successfully used to characterize the thermal behavior of fiber. In comparison with the steady-state experiment, the quasi-steady-state method is insensitive to the radiation heat loss, especially in a relatively large frequency range.

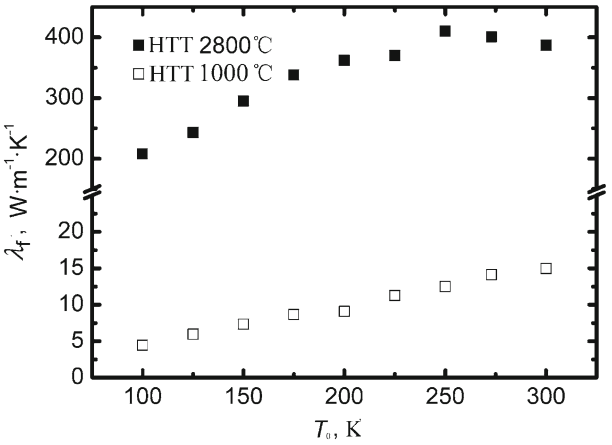

Fig. 4 Temperature dependence of thermal conductivity of carbon fibers

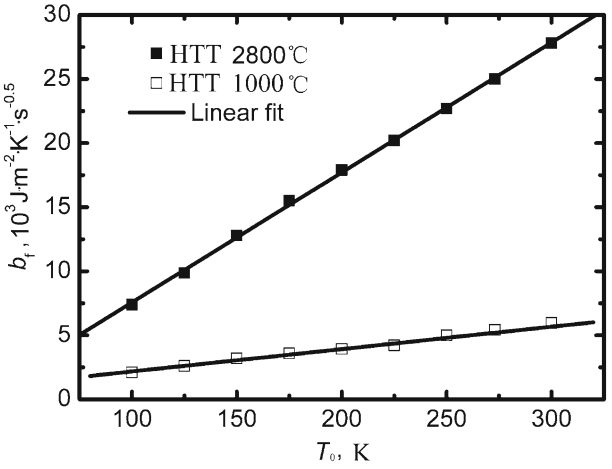

Fig. 5 Temperature dependence of thermal effusivity of carbon fibers

At room temperature, the thermal effusivity of 2800 °C heat-treated fiber is about five times larger than that of the fiber with low HTT.

Figure 6a shows the temperature dependence of the thermal diffusivity. The thermal diffusivity of 2800 °C heat-treated fiber is found to decrease with increasing temperature, and is much larger than that of the other sample. In contrast, the thermal diffusivity of 1000 °C heat-treated fiber is nearly temperature independent. The calculated volumetric specific heat is plotted as a function of temperature in Fig. 6b, and is compared with the graphite data [21] with a density of 2.26 g · cm^{-3}. Similar to the temperature behavior observed in the graphite, the specific heats of both fibers increase with increasing temperature. As the HTT increases, the specific heat decreases, and the value of the fiber heat treated at 2800 °C is close to that of graphite. It is well known that the specific heat can be calculated from phonon frequency distributions,

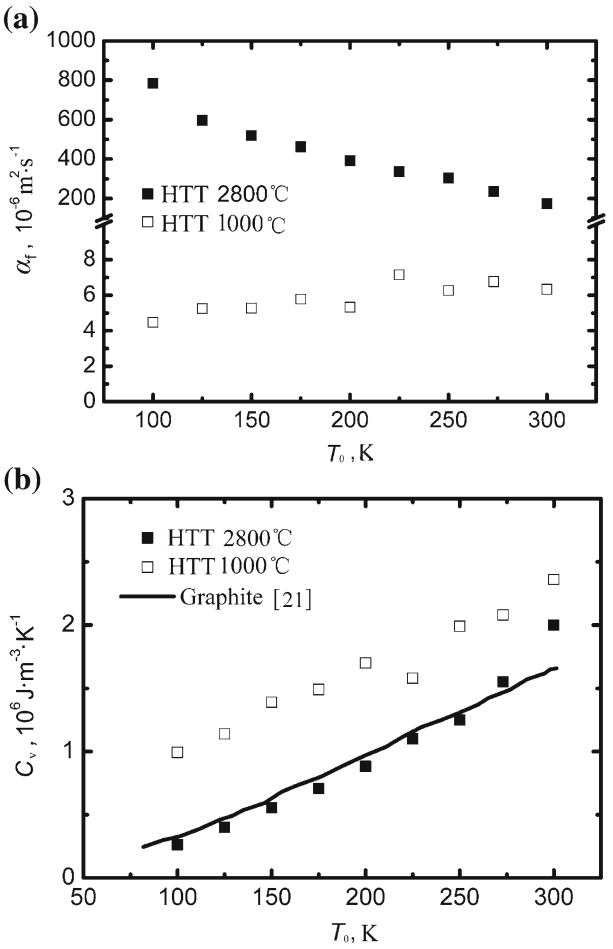

Fig. 6 Calculated (a) thermal diffusivity and (b) volumetric specific heat as a function of temperature

which are related to the lattice vibrations. The crystallite sizes, *Lc* and *La*, increase with increasing HTT, so that more carbon atoms will be linked together by the strong coupled forces, resulting in a small specific heat.

5 Conclusions

The thermal properties of mesophase pitch-based carbon fibers at HTTs of 2800 °C and 1000 °C are systematically investigated from 100 K to 300 K. By imposing both a direct current and an alternating current to the Pt wire in a T type probe, the longitudinal thermal conductivity and thermal effusivity of an individual fiber are obtained, thereby the thermal diffusivity and volumetric specific heat are calculated. The experimental results show that, as the HTT increases, the thermal conductivity and thermal

diffusivity increase, but the specific heat decreases. With the increasing temperature, compared with the carbon fiber heat treated at low temperature, the thermal properties of 2800 °C heat-treated carbon fiber show the following behaviors: (1) the thermal conductivity first increases and then decreases, and reaches a maximum value at about 250 K, (2) the thermal diffusivity has a much larger value and decreases with increasing temperature, and more interestingly, (3) the specific heat is smaller, and is close to that of graphite.

Acknowledgments This work was supported by the National Nature Science Foundation of China (Grant Nos. 50730006 and 50976053).

References

1. I. Michio, F.Y. Kang, *Carbon Materials Sciences and Engineering—From Fundamentals to Applications* (Tsinghua Unviersity Press, Beijing China, 2006)
2. L. Piraux, B. Nysten, A. Haquenne, J.-P. Issi, M.S. Dresselhaus, M. Endo, Solid State Commun. **50**, 697 (1984)
3. H.O. Pierson, *Handbook of Carbon, Graphite, Diamond, and Fullerenes: Properties, Processing and Applications* (Noyes Publications, Park Ridge, New Jersey, 1993)
4. J. Heremans, I. Rahim, M.S. Dresselhaus, Phys. Rev. B **32**, 6742 (1985)
5. T. Yamane, S.-I. Katayama, M. Todoki, J. Appl. Phys. **80**, 4358 (1996)
6. N.C. Gallego, D.D. Edie, B. Nysten, J.P. Issi, J.W. Treleaven, G.V. Deshpande, Carbon **38**, 1003 (2000)
7. X. Zhang, S. Fujiiwara, M. Fujii, Int. J. Thermophys. **21**, 965 (2000)
8. L.M. Manocha, A. Warrier, S. Manocha, D. Sathiyamoorthy, S. Banerjee, Carbon **44**, 480 (2006)
9. Z.L. Wang, D.W. Tang, W.G. Zhang, J. Phys. D: Appl. Phys. **40**, 4686 (2007)
10. C. Pradere, J.C. Batsale, J.M. Goyheneche, R. Pailler, S. Dilhaire, Carbon **47**, 737 (2009)
11. Y.-R. Rhim, D. Zhang, M. Rooney, D.C. Nagle, D.H. Fairbrother, C. Herman, D.G. Drewry, Carbon **48**, 31 (2009)
12. J.L. Wang, M. Gu, X. Zhang, Y. Song, J. Phys. D: Appl. Phys. **42**, 105502 (2009)
13. J.L. Wang, M. Gu, X. Zhang, G.P. Wu, Rev. Sci. Instrum. **80**, 076107 (2009)
14. B. Rosalind, E. Franklin, Proc. R. Soc. A **209**, 196 (1951)
15. T. Hamada, M. Furuyama, Y. Sajiki, T. Tomioka, J. Mater. Res. **5**, 570 (1990)
16. A.K. Kercher, D.C. Nagle, Carbon **41**, 15 (2003)
17. D.G. Cahill, Rev. Sci. Instrum. **61**, 802 (1990)
18. L. Lu, W. Yi, D.L. Zhang, Rev. Sci. Instrum. **72**, 2996 (2001)
19. J.L. Wang, M. Gu, B. Song, X. Zhang, Int. J. Thermophys. **31**, 1145 (2010)
20. B.T. Kelly, *Physics of Graphite* (Applied Science Publishers, London, 1981), pp. 223–252
21. W. de Sorbo, W.W. Tyler, J. Chem. Phys. **21**, 1660 (1953)